VIP Nonlinear Optics Very Important Paper

International Edition: DOI: 10.1002/anie.201802058
German Edition: DOI: 10.1002/ange.201802058

$SrB_5O_7F_3$ Functionalized with $[B_5O_9F_3]^{6-}$ Chromophores: Accelerating the Rational Design of Deep-Ultraviolet Nonlinear Optical Materials

*Miriding Mutailipu[+], Min Zhang[+], Bingbing Zhang, Liying Wang, Zhihua Yang, Xin Zhou, and Shilie Pan**

Abstract: *Fluorooxoborates, benefiting from the large optical band gap, high anisotropy, and ever-greater possibility to form non-centrosymmetric structures activated by the large polarization of $[BO_xF_{4-x}]^{(x+1)-}$ building blocks, have been considered as the new fertile fields for searching the ultraviolet (UV) and deep-UV nonlinear optical (NLO) materials. Herein, we report the first asymmetric alkaline-earth metal fluorooxoborate $SrB_5O_7F_3$, which is rationally designed by taking the classic $Sr_2Be_2B_2O_7$ (SBBO) as a maternal structure. Its $[B_5O_9F_3]^{6-}$ fundamental building block with near-planar configuration composed by two edge-sharing $[B_3O_6F_2]^{5-}$ rings in $SrB_5O_7F_3$ has not been reported in any other borates. Solid state ^{19}F and ^{11}B magic-angle spinning NMR spectroscopy verifies the presence of covalent B–F bonds in $SrB_5O_7F_3$. Property characterizations reveal that $SrB_5O_7F_3$ possesses the optical properties required for deep-UV NLO applications, which make $SrB_5O_7F_3$ a promising crystal that could produce deep-UV coherent light by the direct SHG process.*

The ever-growing application of the deep-ultraviolet (deep-UV, $\lambda < 200$ nm) nonlinear optical (NLO) materials[1] in various fields requires searching for more candidates to generate deep-UV lasers through the direct second-harmonic generation (SHG) method.[2] Remarkably, $KBe_2BO_3F_2$ (KBBF) is the sole material that could practically generate the 177.3 nm coherent laser by a direct SHG method. The infinite $^2_\infty[Be_2BO_3F_2]^-$ single layers in KBBF provide a relatively large SHG coefficient ($d_{11} = 0.47\ pm\ V^{-1}$) and a sufficient birefringence ($\Delta n = 0.077$@1064 nm).[3] To improve the layering tendency of KBBF, $Sr_2Be_2B_2O_7$ (SBBO)[1a] was rationally designed and synthesized, it preserves the merits of the optical properties of KBBF and thus is one of the most promising candidates for frequency doubling into the deep-UV region. However, the poor structural stability of SBBO limits its application. The instability is caused by the cohesion forces between the $^2_\infty[Be_2B_2O_7]^{4-}$ layers.[4]

Against this background, it is necessary to commence systematic studies aiming at improving the performances of KBBF and SBBO. Among them, the structure-oriented design strategy, that is, making structural modifications based on the favorable layered structures of KBBF or SBBO, has been shown to be an effective way. This strategy promoted the discovery and development of several beryllium borates $Na_2Be_4B_4O_{11}$,[5] $NaSr_3Be_3B_3O_9F_4$[6] and beryllium-free borates $Li_4Sr(BO_3)_2$,[7] $BaAlBO_3F_2$,[8] $Cs_3Zn_6B_9O_{21}$[9,10] with balanced optical properties. Even so, an ideal candidate is still needed.

Recently, our group has concentrated on introducing fluorine into the B–O clusters to obtain fluorooxoborates, and in better understanding the microscopic mechanisms of $[BO_xF_{4-x}]^{(x+1)-}$ basic units on improving the birefringence.[11] Consequently, several alkali-metal fluorooxoborates, including $Li_2B_6O_9F_2$,[11a] $Na_2B_6O_9F_2$,[11b] as well as AB_4O_6F (A = NH_4, Cs) series[11c,d] were reported as the ideal candidates for the deep-UV NLO or birefringent materials. Their superior properties result from the improved anisotropic polarizabilities of their B–O/F fundamental building blocks (FBBs). The FBB of $Li_2B_6O_9F_2$ is $[B_6O_{11}F_2]^{6-}$ composed of non-coplanar $[B_5O_{10}]^{5-}$ and $[BO_2F_2]^{3-}$ units.[11a,12] While the $[B_3O_6]^{3-}$ units in $[B_4O_8F]^{5-}$ FBB of AB_4O_6F series are near-planar and aligned, which give rise to a relatively large SHG response and a sufficient birefringence due to the delocalized π-conjugated bonds.[11c,d] Also very recently, centrosymmetric $BaB_4O_6F_2$[13a] was reported as the first alkaline-earth fluorooxoborate, which shares a similar $[B_4O_8F_2]^{6-}$ FBB with the AB_4O_6F series. Besides, more B-O/F FBBs in other related fluorooxoborates, such as $[B_3O_5F_3]^{4-}$, $[B_3O_6F_6]^{9-}$, $[B_3O_8F]^{8-}$, as well as $[B_6O_9F_2]^{2-}$, were reported as being vital constituents in borates-based structural chemistry.[14] Therefore, enriching the structural diversity of FBBs and making it in favorable configurations seems important.

Herein, by taking the classic SBBO as a maternal structure, we expect to substitute the BeO_4 units by $[BO_xF_{4-x}]^{(x+1)-}$ units to create new beryllium-free strontium fluorooxoborates, which is expected to not only eliminate the toxicity and structural instability issues but also preserve the NLO-favorable structural features. Thus, systematic explora-

[*] M. Mutailipu,[+] Dr. M. Zhang,[+] Dr. B. Zhang, Prof. Z. Yang, Prof. S. Pan
CAS Key Laboratory of Functional Materials and Devices for Special Environments; Xinjiang Technical Institute of Physics & Chemistry, CAS; Xinjiang Key Laboratory of Electronic Information Materials and Devices
40-1 South Beijing Road, Urumqi 830011 (China)
E-mail: slpan@ms.xjb.ac.cn
M. Mutailipu[+]
University of Chinese Academy of Sciences
Beijing 100049 (China)
Prof. L. Wang, Prof. X. Zhou
Key Laboratory of Magnetic Resonance in Biological Systems, State Key Laboratory of Magnetic Resonance and Atomic and Molecular Physics, National Center for Magnetic Resonance in Wuhan, Wuhan Institute of Physics and Mathematics, CAS
Wuhan 430071 (China)
[+] These authors contributed equally to this work.
Supporting information and the ORCID identification number(s) for the author(s) of this article can be found under: https://doi.org/10.1002/anie.201802058.

tions on the Sr–B–O/F system lead to the discovery of a new strontium fluorooxoborate, $SrB_5O_7F_3$ (SBF), which is the first case of an asymmetric alkaline-earth metal fluorooxoborate and contains the $[B_5O_9F_3]^{6-}$ FBB which has not been reported in any other systems. In addition, SBF has the optical properties required for deep-UV NLO applications, including a short deep-UV cutoff edge, a large SHG response, and a suitable birefringence, which strongly suggest that SBF is a potential deep-UV NLO material.

SBF crystallizes in an orthorhombic crystal system with non-centrosymmetric space group of $Cmc2_1$ (Table S1 in the Supporting Information). As depicted in Figure 1, the structure of SBF features two dimensional (2D) zigzag $^2_\infty[B_5O_7F_3]^{2-}$ layers with the Sr^{2+} cations residing in the

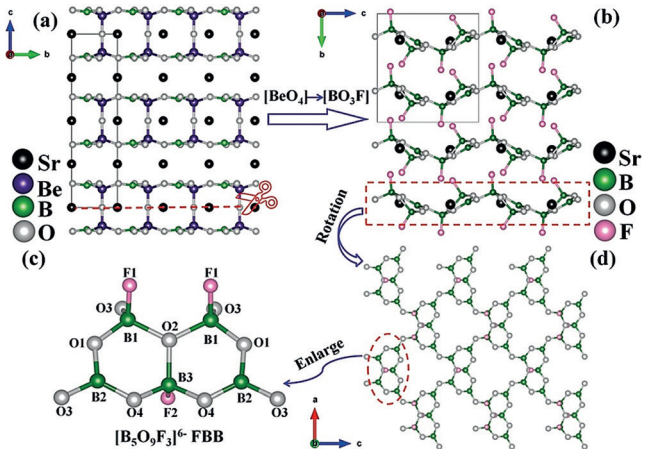

Figure 1. a),b) The structural evolution from $Sr_2Be_2B_2O_7$ to $SrB_5O_7F_3$ by substituting $[BeO_4]$ for $[BO_3F]^{4-}$ units. c) The $[B_5O_9F_3]^{6-}$ fundamental building block of $SrB_5O_7F_3$. d) The two-dimensional $^2_\infty[B_5O_7F_3]^{2-}$ single layer extending in the *ac* plane.

layers. The asymmetric unit of SBF consists of one Sr atom, three B atoms, four O atoms, and two F atoms (Tables S2, S3). In terms of the B–O/F polyanionic structure, the B(2) and B(1,3) atoms are three- and four- coordinated with the oxygen/fluorine atoms to give the triangular $[B(2)O_3]^{3-}$ and tetrahedral $[B(1,3)O_3F]^{4-}$ basic units, respectively (Table S4 and Figure 1 c). The three crystallographic basic units are enclosed into a $[B_3O_6F_2]^{5-}$ single ring, then two rings further polymerize into a $[B_5O_9F_3]^{6-}$ double ring (Figure 1 c) by sharing the edged B(3)-O(2) bond in $[B(3)O_3F]^{4-}$. The bridge oxygen O(3) atoms act as linkers to yield the 2D zigzag $^2_\infty[B_5O_7F_3]^{2-}$ single layers extending in the *ac* plane (Figure 1 d). Then the adjacent single layers are stacked along the [010] direction in the -AAAA- sequence, and held together via F-Sr-F electrovalent bonds to generate the 2D layered monolithic construction with the large 18-membered ring (MR) channels running along [010] direction (Figure 1 b and Figure S2).

To our knowledge, the naphthalene liked $[B_5O_9F_3]^{6-}$ FBB has never been reported in borate systems. The double rings in $[B_5O_9F_3]^{6-}$ FBB are in near-planar configuration, this is quite different from the other stereoscopic pentaborate FBBs[15] ($[B_5O_{10}]^{5-}$, $[B_5O_{11}]^{7-}$ and $[B_5O_{12}]^{9-}$). Clearly, tetrahedrally coordinate B atoms connect two single rings in the pentaborate FBBs by sharing corners and build stereoscopic configurations (Figure S5). The $[B_5O_9F_3]^{6-}$ FBBs with near-planar configuration are more likely to generate large SHG responses and birefringence due to the delocalized π-conjugated bonds, so the high optical performances of SBF are expected.

In addition, the structural evolution from SBBO to SBF is illustrated in Figures 1 a, b, the fluorine atoms act as scissors to "cutoff" the Be–O bonds in the Be_2O_7 dimers and "break" the double layers, meanwhile, the $[BeO_4]^{6-}$ units are replaced by $[BO_3F]^{4-}$ to create a new beryllium-free strontium fluorooxoborate. Structurally, the above evolution strategies can bring more beneficial characteristics: 1) the double layers are pulled down and the cohesion forces between the $^2_\infty[Be_2B_2O_7]^{4-}$ layers is weakened, thus the structure characters are shown to be stable in SBF, which can be verified by the decreased structural convergence factors[16] from SBBO (>0.065)[1a] to SBF (0.0257); 2) the structure of the derivative SBF not only preserves the NLO-favorable structural features but also introduces the $[BO_3F]^{4-}$ units with improved polarizability anisotropies, which is expected to produce a suitable SHG response and birefringence; 3) the replacement of $[BeO_4]^{6-}$ by the $[BO_3F]^{4-}$ units is a step to completely remove the toxicity issues in SBBO. More particularly, the evolution process generates an unprecedented $[B_5O_9F_3]^{6-}$ FBB in which the B–O and B–F bond lengths varying from 1.348(5) to 1.533(5) Å and 1.413(5) to 1.417(7) Å, respectively. Among them, B(1)–O(2) (1.533(5) Å) and B(3)–O(2) (1.525(8) Å) are the two longest B–O bonds in the $[B_5O_9F_3]^{6-}$ FBB (Table S4), showing the unique three coordinated (OB_3) behavior of the O(2) atoms. The similar OB_3 groups and much longer B–O bonds can also be found in other related borates,[17] in which the central O atoms are surrounded by the three tetrahedral $[BO_4]^{5-}$ units to construct $O(BO_4)_3$ clusters. In SBF, the constructed units can be assigned as $O(BO_3F)_3$ (Figure S6). The bond valence sum calculations of the central O(2) atom in $O(BO_3F)_3$ results in the reasonable value of 1.954, which indicates that the unique three coordinated oxygen model is correct.

Although the presence and coordination of fluorine atoms are demonstrated by single-crystal structure analysis, IR spectroscopy (Figure S7), bond valence calculations (Table S2), and energy-dispersive X-ray spectroscopy (Figure S8), we verified the presence of B–F bonds by solid-state NMR spectroscopy. High-resolution, solid-state ^{19}F NMR is a powerful tool to identify and character the local environments of fluorooxoborates at the atomic level. First, a 100 % natural abundance and a high gyromagnetic ratio of the ^{19}F nucleus allow ^{19}F NMR detection with high sensitivity. Second, the wide isotropic chemical-shift range (ca. 200 ppm) of ^{19}F provides good resolution of the resonance peaks either from different bonding configurations or from different molecular conformations. Meanwhile, the boron isotope ^{11}B is a half-integer quadrupole nucleus, and therefore its resonance frequency depends on both the chemical shift and the magnitude of the so-called quadrupolar interaction, which is sensitive to the symmetry of the charge distribution around the nucleus. Hence, solid-state ^{19}F and ^{11}B magic-angle

spinning (MAS) NMR spectroscopy has been performed to verify the presence of covalent B–F bonds in SBF. The ^{19}F and ^{11}B MAS NMR spectra of SBF are shown in Figures 2a,b. In the ^{19}F MAS NMR spectrum (Figure 2a), based on the previous ^{19}F MAS NMR spectra of $BaB_4O_6F_2$ and alkaline-earth metal fluorides by Höppe et al. and Kemnitz and co-workers,[13] the signal at −87.1 ppm was assigned to F nearest

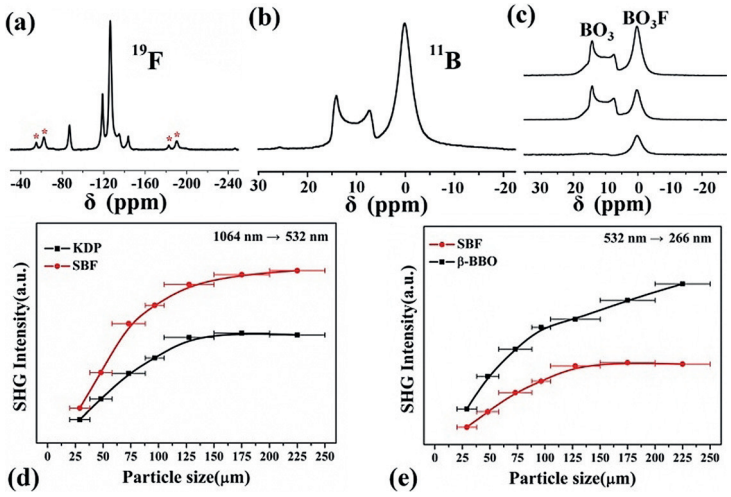

Figure 2. a) ^{19}F-, b) ^{11}B, and c) $^{11}B\{^{19}F\}$-REDOR MAS NMR spectra of $SrB_5O_7F_3$. Asterisks denote spinning sidebands. Powder SHG data for $SrB_5O_7F_3$ at 1064 nm (d) and 532 nm (e) laser radiation.

to Sr and the signals at −118.9, −126.2, −134.9, and −143.7 ppm were assigned to the F in B–F groups (Figure 2a). The different chemical shifts and intensities of F signals are from the different crystallographic sites in the crystal shown in Figure 1c. For ^{11}B MAS NMR spectrum (Figure 2b), in agreement with published data on solid-state ^{11}B NMR,[11e,13a] the broad signal within the range of 5 to 15 ppm can be assigned to B in trigonal planar $[BO_3]^{3-}$ units, whereas the narrow signal at 0.20 ppm can be assigned to the tetrahedral coordinated B atoms, because tetrahedral coordination provides higher local electronic symmetry than that of trigonal coordination. The $^{11}B\{^{19}F\}$-REDOR experiments were performed to establish the B–F bonds for the tetrahedral $[BO_3F]^{4-}$ units and the obtained different spectrum is shown in Figure 2c, which clearly demonstrates that there is tetrahedral coordinated B nuclei with B–F bonds in SBF.

The UV/Vis near-infrared diffuse reflectance spectrum was collected on the polycrystalline sample of SBF (Figure S9). As a result, SBF has no obvious absorption from 180 to 2600 nm and its cutoff edge is lower than 180 nm (corresponding to a large band gap >6.89 eV), indicating a high potential of deep-UV transparency. Such short cut off edge is shorter than or comparable to other Sr-based NLO materials.[7,8,18–20] The much shorter cutoff edge of SBF can be explained form the following structural aspects: 1) All the elemental compositions (Sr, B, O, and F) of SBF are free of d–d or f–f electronic transitions, which is beneficial for giving a good transparency in the UV or even deep-UV spectral region; 2) the non-bonding states of O atoms in the B–O units are effectively eliminated by the introduction of fluorine, resulting in there being no dangling bonds in the structures of SBF; 3) the introduction of F atoms with large electronegativity is beneficial in shifting the cutoff edge to the deep-UV region.[21]

According to the results of SHG measurements under both 1064 and 532 nm fundamental wave laser radiations, the SHG efficiency increases with the increasing particle sizes, indicating that SBF exhibits type **I** phase-matching behavior based on the rules proposed by Kurtz and Perry.[22] Results reveal an SHG efficiency of approximately $1.6\times KH_2PO_4$ (KDP) and $0.50\times\beta$-BaB_2O_4 at 1064 and 532 nm, respectively, in the particle size range of 200–250 μm (Figures 2d,e). And such large SHG responses make SBF possible to be applied as NLO materials and the values are also comparable to other UV NLO materials.[3,5,16,18,23] Besides, we also calculated the second-order NLO coefficients d_{ij} based on the first-principles calculation.[24] The space group of SBF is $Cmc2_1$, which belongs to the class $mm2$ point group and has only three non-vanishing independent SHG tensors ($d_{31}=d_{15}=0.91\ pm\ V^{-1}$, $d_{32}=d_{24}=-0.37\ pm\ V^{-1}$, and $d_{33}=-0.71\ pm\ V^{-1}$). Among them, d_{31} and d_{33} are approximately two times that of KDP ($d_{36}=0.39\ pm\ V^{-1}$), which is consistent with the experimental results.

The SHG-weighted electron density analysis was performed to explain the donation of individual atoms in SBF to the SHG effect in real space.[25] We only consider the VE processes since they have dominant contributions to the SHG effects (>90%) in SBF. It can be clearly observed that the non-bonding 2p orbitals of the O and F atoms give the prominent contributions to the SHG response in the VB. While in the CB, the anti π orbitals of the $[BO_3]^{3-}$ groups, unique three-connected O(2) atoms as well as the F atoms give more dominant contributions for the SHG effects, revealing the p-(p, π*) "charge-transfer excitation" mechanism in SBF.[26] Thus, when taken together, the $[B_5O_9F_3]^{6-}$ chromophore in SBF can be regarded as the NLO-active microscopic unit.

The calculated refractive indices as a function of different frequencies are shown in Figure S11. As it follows the inequality $n_z-n_y<n_y-n_x$, the results reveal that SBF is a negative biaxial crystal, with the birefringence (Δn) ranging from 0.070@1064 nm to 0.075@400 nm and the values are comparable to KBBF (0.077@1064 nm) and larger than that of SBBO (0.062@589 nm). Moreover, further analysis of refractive-index dispersion based on the calculated refractive indices was carried out to evaluate the phase-matching ability. As a result, the shortest SHG phase-matching wavelength of SBF (Figure 3b and Figure S12) is down to approximately 180 nm, which is shorter than that of the calculated values of SBBO (ca. 200 nm). This indicates SBF has potential to generate the deep-UV coherent light by a direct SHG process.

In summary, the first asymmetric alkaline-earth fluoroxoborate SBF was structurally designed following the strategy of fluorine-introduction in borates by taking the classic SBBO as the parent structure. This beryllium-free borate presents the first case of a $[B_5O_9F_3]^{6-}$ FBB and features NLO favorable

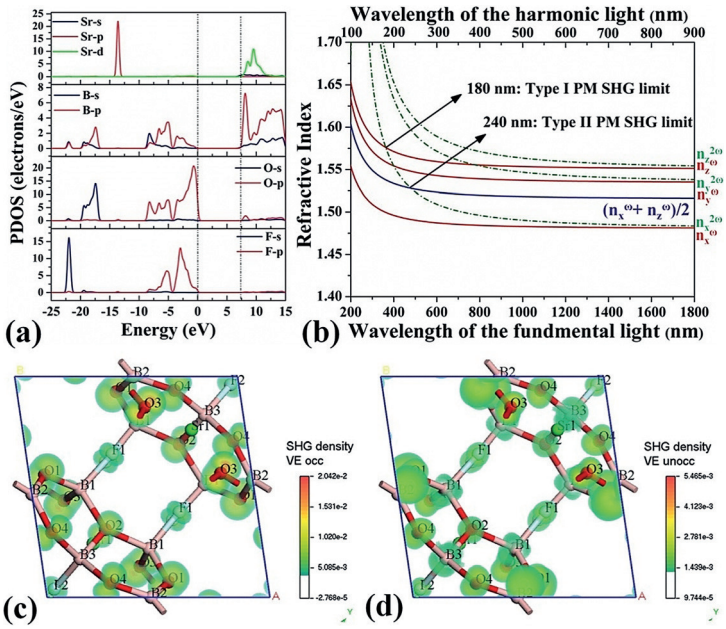

Figure 3. The projected density of states (a), calculated refractive index dispersion curves (b) of $SrB_5O_7F_3$. The SHG density maps of the occupied (c) and unoccupied (d) orbitals of the largest tensor (d_{31}) in VE process.

$^2_\infty[B_5O_7F_3]^{2-}$ single layers, which preserve the structural merits of SBBO. In this way, the most intractable issues of SBBO including toxicity and structural instability problems are avoided in SBF by this design strategy. More importantly, SBF has the optical properties required for deep-UV NLO applications, including a deep-UV transparency (< 180 nm), a sufficiently large SHG response of about 1.6× KDP@1064 nm, a suitable birefringence (0.07@1064 nm), and a deep-UV SHG phase-matching wavelength (ca. 180 nm; Table S5), thus these properties make SBF a promising NLO crystal that could produce deep-UV coherent light by the direct SHG process.

Acknowledgements

This work was financially supported by the Natural Science Foundation of China (Grant Nos. 21501194, 51425206, 81625011, 51702356, 91622107), National Key Research Project (Grant No. 2016YFB0402104), National National Basic Research Program of China (Grant No. 2014CB648400), West Light Foundation of the Chinese Academy of Sciences (Grant No. 2016-YJRC-2).

Conflict of interest

The authors declare no conflict of interest.

Keywords: borates · deep-ultraviolet · fluorooxoborate · functionalized chromophore · nonlinear optical materials

How to cite: *Angew. Chem. Int. Ed.* **2018**, *57*, 6095–6099
Angew. Chem. **2018**, *130*, 6203–6207

[1] a) C. T. Chen, Y. B. Wang, B. C. Wu, K. C. Wu, W. L. Zeng, L. H. Yu, *Nature* **1995**, *373*, 322–324; b) T. T. Tran, H. W. Yu, J. M. Rondinelli, K. R. Poeppelmeier, P. S. Halasyamani, *Chem. Mater.* **2016**, *28*, 5238–5258; c) F. Kong, S. P. Huang, Z. M. Sun, J. G. Mao, W. D. Cheng, *J. Am. Chem. Soc.* **2006**, *128*, 7750–7751; d) C. T. Chen, Y. B. Wang, Y. N. Xia, B. C. Wu, D. Y. Tang, K. C. Wu, W. R. Zeng, L. H. Yu, L. F. Mei, *J. Appl. Phys.* **1995**, *77*, 2268–2272; e) Q. Wei, J. J. Wang, C. He, J. W. Cheng, G. Y. Yang, *Chem. Eur. J.* **2016**, *22*, 10759–10762; f) G. Sohr, N. Ciaghi, M. Schauperl, K. Wurst, K. R. Liedl, H. Huppertz, *Angew. Chem. Int. Ed.* **2015**, *54*, 6360–6363; *Angew. Chem.* **2015**, *127*, 6458–6461.

[2] a) K. M. Ok, *Acc. Chem. Res.* **2016**, *49*, 2774–2785; b) T. T. Tran, N. Z. Koocher, J. M. Rondinelli, P. S. Halasyamani, *Angew. Chem. Int. Ed.* **2017**, *56*, 2969–2973; *Angew. Chem.* **2017**, *129*, 3015–3019; c) G. H. Zou, C. S. Lin, H. Jo, G. Nam, T. S. You, K. M. Ok, *Angew. Chem. Int. Ed.* **2016**, *55*, 12078–12082; *Angew. Chem.* **2016**, *128*, 12257–12261; d) Q. Huang, L. J. Liu, X. Y. Wang, R. K. Li, C. T. Chen, *Inorg. Chem.* **2016**, *55*, 12496–12499; e) M. Mutailipu, Z. Q. Xie, X. Su, M. Zhang, Y. Wang, Z. H. Yang, M. Janjua, S. L. Pan, *J. Am. Chem. Soc.* **2017**, *139*, 18397–18405; f) T. L. Chao, W. J. Chang, S. H. Wen, Y. Q. Lin, B. C. Chang, K. H. Lii, *J. Am. Chem. Soc.* **2016**, *138*, 9061–9064.

[3] a) C. T. Chen, Z. Y. Xu, D. Q. Deng, J. Zhang, G. K. L. Wong, B. C. Wu, N. Ye, D. Y. Tang, *Appl. Phys. Lett.* **1996**, *68*, 2930–2932; b) D. Cyranoski, *Nature* **2009**, *457*, 953–957; c) C. T. Chen, *Opt. Mater.* **2004**, *26*, 425–429.

[4] X. Y. Meng, X. H. Wen, G. L. Liu, *J. Korean Phys. Soc.* **2008**, *52*, 1277–1280.

[5] H. W. Huang, L. J. Liu, S. F. Jin, W. J. Yao, Y. H. Zhang, C. T. Chen, *J. Am. Chem. Soc.* **2013**, *135*, 18319–18322.

[6] H. W. Huang, J. Y. Yao, Z. S. Lin, X. Y. Wang, R. He, W. J. Yao, N. X. Zhai, C. T. Chen, *Angew. Chem. Int. Ed.* **2011**, *50*, 9141–9144; *Angew. Chem.* **2011**, *123*, 9307–9310.

[7] S. G. Zhao, P. F. Gong, L. Bai, X. Xu, S. Q. Zhang, Z. H. Sun, Z. S. Lin, M. C. Hong, C. T. Chen, J. H. Luo, *Nat. Commun.* **2014**, *5*, 4019–4026.

[8] Z. G. Hu, M. Yoshimura, Y. Mori, T. Sasaki, *J. Cryst. Growth* **2004**, *260*, 287–290.

[9] S. G. Zhao, J. Zhang, S. Q. Zhang, Z. H. Sun, Z. S. Lin, Y. C. Wu, M. H. Hong, J. H. Luo, *Inorg. Chem.* **2014**, *53*, 2521–2527.

[10] H. W. Yu, H. P. Wu, S. L. Pan, Z. H. Yang, X. L. Hou, X. Su, Q. Jing, K. R. Poeppelmeier, J. M. Rondinelli, *J. Am. Chem. Soc.* **2014**, *136*, 1264–1267.

[11] a) B. B. Zhang, G. Q. Shi, Z. H. Yang, F. F. Zhang, S. L. Pan, *Angew. Chem. Int. Ed.* **2017**, *56*, 3916–3919; *Angew. Chem.* **2017**, *129*, 3974–3977; b) G. Q. Shi, F. F. Zhang, B. B. Zhang, D. W. Hou, X. L. Chen, Z. H. Yang, S. L. Pan, *Inorg. Chem.* **2017**, *56*, 344–350; c) G. Q. Shi, Y. Wang, F. F. Zhang, B. B. Zhang, Z. H. Yang, X. L. Hou, S. L. Pan, K. R. Poeppelmeier, *J. Am. Chem. Soc.* **2017**, *139*, 10645–10648; d) X. F. Wang, Y. Wang, B. B. Zhang, F. F. Zhang, Z. H. Yang, S. L. Pan, *Angew. Chem. Int. Ed.* **2017**, *56*, 14119–14123; *Angew. Chem.* **2017**, *129*, 14307–14311; e) T. Bräuniger, T. Pilz, C. V. Chandran, M. Jansen, *J. Solid State Chem.* **2012**, *194*, 245–249.

[12] T. Pilz, M. Jansen, *Z. Anorg. Allg. Chem.* **2011**, *637*, 2148–2152.

[13] a) S. G. Jantz, F. Pielnhofer, L. V. Wüllen, R. Weihrich, M. J. Schäfer, H. A. Höppe, *Chem. Eur. J.* **2018**, *24*, 443–450; b) M. Heise, G. Scholz, A. Düvel, P. Heitjans, E. Kemnitz, *Solid State Sci.* **2016**, *60*, 65–74.

[14] a) G. Cakmak, J. Nuss, M. Jansen, *Z. Anorg. Allg. Chem.* **2009**, *635*, 631–636; b) T. Pilz, H. Nuss, M. Jansen, *J. Solid State Chem.* **2012**, *186*, 104–108.

[15] E. L. Belokoneva, *Crystallogr. Rep.* **2005**, *11*, 151 – 198.
[16] H. W. Huang, J. Y. Yao, Z. S. Lin, X. Y. Wang, R. He, W. J. Yao, N. X. Zhai, C. T. Chen, *Chem. Mater.* **2011**, *23*, 5457 – 5463.
[17] a) R. Kaindl, G. Sohr, H. Huppertz, *Spectrochim. Acta Part A* **2013**, *116*, 408 – 417; b) G. Al-Ama, E. L. Belokoneva, S. Y. Stefanovich, O. V. Dimitrova, N. N. Mochenova, *Crystallogr. Rep.* **2006**, *51*, 225 – 230.
[18] H. P. Wu, H. W. Yu, S. L. Pan, P. S. Halasyamani, *Inorg. Chem.* **2017**, *56*, 8755 – 8758.
[19] C. D. McMillen, J. T. Stritzinger, J. W. Kolis, *Inorg. Chem.* **2012**, *51*, 3953 – 3955.
[20] N. Yu, S. C. Wang, N. Ye, F. Liang, Z. S. Lin, M. Luo, K. R. Poeppelmeier, *Chem. Mater.* **2016**, *28*, 4563 – 4571.
[21] a) L. Y. Li, G. B. Li, Y. X. Wang, F. H. Liao, J. H. Lin, *Chem. Mater.* **2005**, *17*, 4174 – 4180; b) M. Mutailipu, X. Su, M. Zhang, Z. H. Yang, S. L. Pan, *Inorg. Chem. Front.* **2017**, *4*, 281 – 288.
[22] S. K. Kurtz, T. T. Perry, *J. Appl. Phys.* **1968**, *39*, 3798 – 3813.
[23] N. Ye, W. R. Zeng, B. C. Wu, C. T. Chen, *Proc. SPIE-Int. Soc. Opt. Eng.* **1998**, *3556*, 21 – 23.
[24] M. H. Lee, C. H. Yang, J. H. Jan, *Phys. Rev. B* **2004**, *70*, 235110.
[25] K. H. Hubner, *Neues Jahrb. Mineral. Monatsh.* **1969**, *111*, 335 – 343.
[26] B. B. Zhang, Z. H. Yang, Y. Yang, M. H. Lee, S. L. Pan, J. Qun, X. Su, *J. Mater. Chem. C* **2014**, *2*, 4133 – 4141.

Manuscript received: February 14, 2018
Accepted manuscript online: March 2, 2018
Version of record online: March 2018, 22

